Information Rate Circle in Dirac Quantum Walks: A Geometric Route to Relativistic Kinematics

First Author Name[1] and Second Author Name[1]

[1] *Your Institution/Department*

(Dated: November 29, 2025)

We demonstrate that for one-dimensional Dirac-type quantum cellular automata (QCA), the single-particle unitary evolution obeys an exact geometric conservation law: $v_{\text{ext}}^2(p) + v_{\text{int}}^2(p) = c^2$, where v_{ext} is the group velocity, v_{int} is an internal rate derived from the Bloch-axis geometry, and c is the Lieb-Robinson causal velocity. We term this the "information rate circle," as it represents a partition of the total causal information capacity into spatial propagation and internal quantum processing. Crucially, we establish the operational significance of the internal rate: v_{int} governs the upper bound of coin-position entanglement generation for narrow wave packets, providing a direct link between the geometric constraint and quantum information resources. This geometric constraint also provides a unified kinematic reconstruction of relativistic physics: defining proper time via $\mathrm{d}\tau = (v_{\text{int}}/c)\,\mathrm{d}t$ in the narrow-wave-packet regime, the familiar special-relativistic relations—time dilation, four-velocity normalization, and energy-momentum relation $E^2 = p_{\text{phys}}^2 c^2 + m^2 c^4$ with $m = \hbar\mu/c^2$—emerge naturally in the long-wavelength limit. Our results suggest that relativistic kinematic structure can be viewed as an emergent property of the resource trade-off in discrete quantum information processing.

Introduction.— The origin of spacetime geometry remains one of the deepest questions in fundamental physics. While general relativity treats spacetime as a continuous manifold with metric structure, quantum information theory suggests the universe may be fundamentally discrete, with dynamics governed by local unitary operations on finite-dimensional Hilbert spaces [1–3]. Quantum cellular automata (QCA)—discrete quantum systems with local interactions and finite signal velocity—provide a rigorous framework for "universe as quantum computation," successfully recovering free quantum field theory in appropriate continuum limits [1, 4].

A central puzzle is how the continuous Lorentz symmetry and Minkowski metric of special relativity can emerge from discrete quantum dynamics with no *a priori* spacetime structure. Previous work has shown that Dirac equations arise naturally in QCA models [5–7], typically via asymptotic expansions of the discrete dispersion relation in the long-wavelength limit [1]. Finite signal velocity in quantum lattice systems is rigorously characterized by Lieb–Robinson bounds [8, 9]. However, a simple geometric picture that organizes these discrete structures and their connection to relativistic kinematics has remained implicit.

In this work, we identify such a geometric organizing principle. *Unlike previous works that derive relativistic behavior via continuum approximations, we identify an exact finite-lattice geometric identity that remains valid at all energy scales and momentum modes.* For one-dimensional Dirac-type QCA, the single-step unitary evolution $U(p) = e^{-i\Omega(p)\hat{n}(p)\cdot\vec{\sigma}}$ naturally decomposes the Bloch axis $\hat{n}(p)$ relative to a propagation direction $\hat{d}$. Defining external group velocity $v_{\text{ext}}(p) := c\,\hat{n}\cdot\hat{d}$ and internal rate $v_{\text{int}}(p) := c\,|\hat{n}\times\hat{d}|$ (where $c = a/\Delta t$ is the lattice velocity scale), the unit-norm constraint $|\hat{n}|^2 = 1$ immediately yields

$$v_{\text{ext}}^2(p) + v_{\text{int}}^2(p) = c^2. \tag{1}$$

Mathematically, Eq. (1) is simply the statement that $(\hat{n}\cdot\hat{d})^2 + |\hat{n}\times\hat{d}|^2 = 1$ for any unit vector $\hat{n}$—a trivial geometric identity. We call this the **information rate circle** to emphasize its physical significance: c coincides with the Lieb-Robinson causal velocity (A2), so the identity represents a partition of the total causal capacity between spatial propagation and internal processing.[**?**]

Remarkably, when one defines a proper-time parameter via $\mathrm{d}\tau := (v_{\text{int}}/c)\,\mathrm{d}t$, the familiar relativistic relations—time dilation $\gamma = (\mathrm{d}t/\mathrm{d}\tau)$, four-velocity normalization, and energy-momentum relation $E^2 = p_{\text{phys}}^2 c^2 + m^2 c^4$ with $m = \hbar\mu/c^2$—are recovered in the long-wavelength, narrow-wave-packet limit. This does not constitute an independent derivation of special relativity; rather, it shows that the known Dirac dispersion and relativistic energy-momentum relation can be geometrically organized as consequences of Eq. (1) together with the SU(2) structure of the quantum walk.

The physical significance of this geometric identity rests on two quantitative links to observables:

(i) *Entanglement generation:* We prove that v_{int} controls a rigorous one-step upper bound on coin-position entanglement growth for narrow wave packets (Proposition 1). This establishes v_{int} as the physical scale governing quantum correlation generation, elevating the rate circle from a kinematic curiosity to a constraint on information-theoretic resources.

(ii) *Causal structure:* For this class of nearest-neighbor Dirac QCA, the lattice velocity c coincides with the Lieb-Robinson causal velocity v_{LR} (A2), so that the circle relation is a geometric decomposition of the

light-cone speed into external and internal components.

Together, these results demonstrate that the "information rate" terminology is not merely metaphorical: $v_{\rm int}$ governs the rate of quantum information generation, while c sets the causal limit on both spatial propagation and internal processing.

I. MODEL AND AXIOMS

A. Discrete-Time Dirac Quantum Walk

We consider a discrete-time quantum walk on the one-dimensional lattice $\Lambda = \mathbb{Z}$, with each site $x \in \mathbb{Z}$ carrying a two-dimensional "coin" Hilbert space $\mathcal{H}_x \cong \mathbb{C}^2$. The total single-particle Hilbert space is $\mathcal{H} = \ell^2(\mathbb{Z}) \otimes \mathbb{C}^2$, where $\ell^2(\mathbb{Z})$ describes the position degree of freedom and $\mathbb{C}^2$ describes the internal spin-like degree of freedom.

Time evolution proceeds in discrete steps of duration Δt, governed by a unitary operator U acting on $\mathcal{H}$. We impose three structural axioms on this quantum walk:

A1 (Discrete–Unitary–Local): Evolution given by quasilocal unitary operator U acting on finite-dimensional cells with bounded interaction range.

A2 (Finite Light Cone): Lieb–Robinson bound holds: for local operators A, B separated by distance d,

$$\|[\alpha_t(A), B]\| \le C\|A\|\|B\|e^{-\mu(d - v_{\rm LR}|t|)}, \tag{2}$$

where $\alpha_t(A) = U^t A U^{-t}$ and $v_{\rm LR} > 0$ is the Lieb-Robinson velocity [8, 9]. For the class of nearest-neighbor, translation-invariant Dirac-type QCAs considered here (A3), the Lieb-Robinson velocity $v_{\rm LR}$ coincides with the single-particle massless group velocity $c = a/\Delta t$. This can be established by noting that: (i) the LR bound for nearest-neighbor unitary circuits gives $v_{\rm LR} = \mathcal{O}(a/\Delta t)$ [9], and (ii) the massless mode ($\mu = 0$) saturates $|v_{\rm ext}| = c$ from the dispersion relation. Throughout this paper we use c to denote this common velocity scale.

A3 (Dirac Effective Mode): Low-energy sector contains translation-invariant mode with two-component internal structure whose single-step update operator in momentum representation is

$$U(p) = C(\mu)\, T(p) = e^{-i\mu\Delta t\, \hat{m}\cdot\vec{\sigma}} e^{-ipa\, \hat{d}\cdot\vec{\sigma}}, \tag{3}$$

where a is lattice spacing, Δt is time step, μ is a microscopic frequency parameter (with dimensions of inverse time), p is the lattice wave number (inverse length), $\vec{\sigma} = (\sigma_x, \sigma_y, \sigma_z)$ is the vector of Pauli matrices, and $\hat{m}, \hat{d} \in S^2$ are fixed unit vectors satisfying $\hat{m} \cdot \hat{d} = 0$. Here $\hat{d}$ specifies the "propagation direction operator" and $\hat{m}$ specifies the "mass operator direction." The orthogonality condition $\hat{m} \perp \hat{d}$ ensures the Dirac-type anticommutation structure analogous to the continuum Dirac Hamiltonian $\mu\sigma_x + cp\sigma_z$. Throughout this paper we take $c = a/\Delta t$ as the natural velocity scale of the QCA (saturated by massless modes), with c kept explicit in all expressions.

Basis-independent formulation.— For any orthogonal pair $(\hat{m}, \hat{d})$, there exists a global SU(2) transformation W such that $W(\hat{m}\cdot\vec{\sigma})W^\dagger = \sigma_x$ and $W(\hat{d}\cdot\vec{\sigma})W^\dagger = \sigma_z$. Thus Eq. (3) encompasses all Dirac-type quantum walks related by coin-space rotations. The standard choice $\hat{m} = (1,0,0)$, $\hat{d} = (0,0,1)$ recovers the familiar form $U(p) = e^{-i\mu\Delta t\sigma_x} e^{-ipa\sigma_z}$ [5, 6]. This assumption singles out the standard class of translation-invariant two-component Dirac quantum walks, which captures the low-energy sector of several QCA constructions but does not exhaust all possible Dirac-type QCAs.

Dispersion Relation and Bloch Structure.— The update operator (3) is an element of SU(2) and can be written in Bloch form:

$$U(p) = e^{-i\Omega(p)\, \hat{n}(p)\cdot\vec{\sigma}}, \tag{4}$$

where $\Omega(p) \in [0, \pi]$ is the characteristic angle and $\hat{n}(p) \in S^2$ is the Bloch unit vector.

Using the SU(2) multiplication formula [10]

$$e^{-i\alpha\, \hat{a}\cdot\vec{\sigma}} e^{-i\beta\, \hat{b}\cdot\vec{\sigma}} = e^{-i\gamma\, \hat{c}\cdot\vec{\sigma}}, \tag{5}$$

with

$$\cos\gamma = \cos\alpha\cos\beta - (\hat{a}\cdot\hat{b})\sin\alpha\sin\beta, \tag{6}$$

we take $\alpha = \mu\Delta t$, $\beta = pa$, $\hat{a} = \hat{m}$, $\hat{b} = \hat{d}$ (with $\hat{m}\cdot\hat{d} = 0$) to obtain:

Theorem 1 (Dirac–QCA Dispersion): For the one-dimensional Dirac quantum walk defined in Eq. (3), the characteristic angle $\Omega(p)$ satisfies

$$\cos\big(\Omega(p)\big) = \cos(\mu\Delta t)\cos(pa). \tag{7}$$

The Bloch axis satisfies

$$\hat{n}(p)\sin\Omega(p) = \hat{m}\sin(\mu\Delta t)\cos(pa) + \hat{d}\sin(pa)\cos(\mu\Delta t) - (\hat{m}\times\hat{d})\sin(\mu \tag{8}$$

Natural orthogonal frame.— To extract component expressions, we introduce the right-handed orthonormal basis

$$\hat{e}_1 := \hat{m}, \quad \hat{e}_2 := -\hat{m}\times\hat{d}, \quad \hat{e}_3 := \hat{d}. \tag{9}$$

This basis has clear physical meaning: $\hat{e}_1$ is the mass operator direction, $\hat{e}_3$ is the propagation direction, and $\hat{e}_2$ is orthogonal to both, forming the "mass plane" $\mathcal{P} := \mathrm{span}\{\hat{e}_1, \hat{e}_2\}$. Writing $\hat{n}(p) = \sum_{j=1}^{3} n_j(p)\, \hat{e}_j$, Eq. (8) yields

$$n_1(p) = \frac{\sin(\mu\Delta t)\cos(pa)}{\sin\Omega(p)}, \tag{10}$$

$$n_2(p) = \frac{\sin(\mu\Delta t)\sin(pa)}{\sin\Omega(p)}, \tag{11}$$

$$n_3(p) = \frac{\cos(\mu\Delta t)\sin(pa)}{\sin\Omega(p)}. \tag{12}$$

In what follows we restrict to the branch of $\Omega(p)$ continuous at $p = 0$ with $\Omega(0) \approx \mu\Delta t$, corresponding to the low-energy Dirac sector.

Information Rate Circle.— Define the angular frequency $\omega(p) := \Omega(p)/\Delta t$. The **external group velocity** is

$$v_{\text{ext}}(p) := \frac{\mathrm{d}\omega}{\mathrm{d}p}. \tag{13}$$

From the dispersion relation (7), differentiating with respect to p yields

$$-\sin\Omega\,\frac{\mathrm{d}\Omega}{\mathrm{d}p} = -\cos(\mu\Delta t)\sin(pa)\cdot a, \tag{14}$$

so that

$$v_{\text{ext}}(p) = \frac{a}{\Delta t}\,\frac{\cos(\mu\Delta t)\sin(pa)}{\sin\Omega(p)} = c\,n_3(p) = c\,\hat{n}(p)\cdot\hat{d}, \tag{15}$$

where we used Eq. (12), $c = a/\Delta t$, and $\hat{d} = \hat{e}_3$. Thus the external velocity is the projection of the Bloch axis onto the propagation direction $\hat{d}$, expressed in a completely basis-independent form.

We now introduce the complementary **internal rate**. In the natural frame, we have

$$\hat{n}(p)\times\hat{d} = (n_1\hat{e}_1+n_2\hat{e}_2+n_3\hat{e}_3)\times\hat{e}_3 = n_1(\hat{e}_1\times\hat{e}_3)+n_2(\hat{e}_2\times\hat{e}_3). \tag{16}$$

Using the right-handed basis relations $\hat{e}_1 \times \hat{e}_3 = -\hat{e}_2$ and $\hat{e}_2 \times \hat{e}_3 = \hat{e}_1$, we obtain

$$\hat{n}(p) \times \hat{d} = -n_1\hat{e}_2 + n_2\hat{e}_1, \quad \Rightarrow \quad |\hat{n}(p) \times \hat{d}| = \sqrt{n_1^2 + n_2^2}. \tag{17}$$

We define the internal rate as

$$v_{\text{int}}(p) := c\,|\hat{n}(p) \times \hat{d}| = c\,\frac{\sin(\mu\Delta t)}{\sin\Omega(p)}, \tag{18}$$

where the last equality follows from Eqs. (10)–(11). This is a completely basis-independent geometric quantity: the magnitude of the cross product $\hat{n} \times \hat{d}$ measures how much of the Bloch axis lies in the plane perpendicular to the propagation direction.

Clarification: $v_{\text{int}}(p)$ is a **geometric quantity constructed from the generator** $U(p)$, not the instantaneous precession speed of a prepared coin state. The cross product $\hat{n} \times \hat{d}$ measures the component of the Bloch axis perpendicular to the propagation direction—precisely the "mass plane" projection. The physical interpretation becomes clear in the continuum limit: using the emergent relativistic dispersion we will show below that v_{int}/c coincides with the standard ratio of rest energy to total energy, $\mathrm{d}\tau/\mathrm{d}t$, for a relativistic particle.

Theorem 2 (Information Rate Circle, Basis-Independent): For any Dirac-type quantum walk satisfying A1–A3, with $\hat{m} \cdot \hat{d} = 0$, the Bloch axis $\hat{n}(p)$ and propagation direction $\hat{d}$ satisfy

$$\frac{v_{\text{ext}}(p)}{c} = \hat{n}(p)\cdot\hat{d}, \qquad \frac{v_{\text{int}}(p)}{c} = |\hat{n}(p)\times\hat{d}|, \tag{19}$$

and the external and internal rates satisfy the exact identity

$$v_{\text{ext}}^2(p) + v_{\text{int}}^2(p) = c^2 \tag{20}$$

for all momentum modes $p \in [-\pi/a, \pi/a]$ with $\sin\Omega(p) \neq 0$. The relation extends by continuity to the isolated points where $\sin\Omega(p) = 0$.

Proof: The geometric definitions (15)–(18) directly yield Eq. (19). For any unit vector $\hat{n}$ and any fixed direction $\hat{d}$, the decomposition

$$\hat{n} = (\hat{n}\cdot\hat{d})\hat{d} + [\hat{n} - (\hat{n}\cdot\hat{d})\hat{d}] \tag{21}$$

splits $\hat{n}$ into parallel and perpendicular components. Taking the squared norm and using the vector identity $|\hat{n}\times\hat{d}|^2 = |\hat{n}|^2|\hat{d}|^2 - (\hat{n}\cdot\hat{d})^2$, we obtain

$$(\hat{n}\cdot\hat{d})^2 + |\hat{n}\times\hat{d}|^2 = 1. \tag{22}$$

Multiplying by c^2 immediately yields Eq. (20). □

Universality and geometric interpretation.— Theorem 2 is *completely basis-independent*: the dot product $\hat{n}\cdot\hat{d}$ and cross product magnitude $|\hat{n}\times\hat{d}|$ are geometric invariants, independent of any choice of coordinates or Pauli-matrix representation. The information rate circle is a fundamental property of the SU(2) structure: the Bloch axis $\hat{n}(p)$ must lie on the unit sphere, and its decomposition relative to the propagation axis $\hat{d}$ uniquely determines the split between external and internal rates. This holds for *any* orthogonal pair $(\hat{m}, \hat{d})$, encompassing all Dirac-type QCAs related by global coin-space rotations.

This identity reveals a fundamental constraint: the total information update rate c of the QCA is conserved but redistributed between external propagation and internal processing depending on momentum mode.

Operational interpretation of the budget c.— Crucially, the constant c on the right-hand side of Eq. (20) is not merely a lattice parameter but the rigorous limit on information propagation velocity. For this nearest-neighbor unitary evolution, $c = a/\Delta t$ coincides with the Lieb-Robinson velocity v_{LR} (see A2). Thus, the rate circle identity implies that the total causal capacity of the local interaction is conserved but dynamically allocated: strictly massless modes utilize the full capacity for signal transmission ($v_{\text{ext}} = v_{\text{LR}}$, $v_{\text{int}} = 0$), whereas massive modes divert a portion of this capacity ($v_{\text{int}} > 0$) to drive internal coin-space dynamics, manifesting physically as rest mass and entanglement generation (Sec. III.B). This dual role of c as both lattice velocity and causal limit provides the operational justification for the term "information rate circle."

Emergence of Special Relativity.— Given the rate circle (20), it is natural to parametrize worldlines in terms of a time variable τ whose rate is controlled by the internal fraction v_{int}/c. For each momentum mode we **define**

$$\mathrm{d}\tau := \frac{v_{\text{int}}}{c}\,\mathrm{d}t, \tag{23}$$

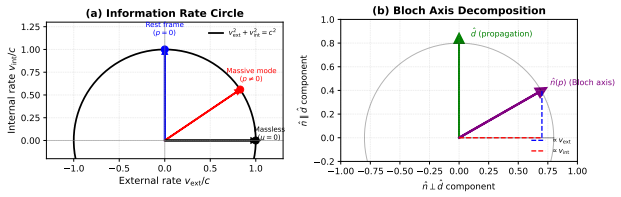

FIG. 1. Geometric visualization of the information rate circle. (a) The conservation law $v_{\text{ext}}^2 + v_{\text{int}}^2 = c^2$ constrains all momentum modes to lie on a circle of radius c (the Lieb-Robinson velocity). Example modes shown: rest frame (blue, $p = 0$, maximum v_{int}), generic massive mode (red), and massless mode (black, on horizontal axis with $v_{\text{int}} = 0$). (b) Bloch sphere representation: the Bloch axis $\hat{n}(p)$ (purple) decomposes relative to the propagation direction $\hat{d}$ (green) into parallel component (proportional to v_{ext}, blue dashed) and perpendicular component (proportional to v_{int}, red dashed). The unit-norm constraint $|\hat{n}| = 1$ enforces the circle constraint.

where $v_{\text{int}}(p)$ is evaluated at a fixed momentum p.[**?**] Upon interpreting $v := v_{\text{ext}}(p)$ as the physical velocity in the continuum limit and using $v_{\text{int}} = \sqrt{c^2 - v^2}$ from Eq. (20), we obtain

$$\frac{\mathrm{d}\tau}{\mathrm{d}t} = \frac{v_{\text{int}}}{c} = \sqrt{1 - \frac{v^2}{c^2}}. \tag{24}$$

This reproduces the standard Lorentz time dilation formula. The parameter τ is thus identified with Minkowskian proper time along the wave packet center trajectory, and we have the Lorentz factor

$$\gamma = \frac{\mathrm{d}t}{\mathrm{d}\tau} = \frac{1}{\sqrt{1 - v^2/c^2}}. \tag{25}$$

The **four-velocity** is defined as

$$u^\mu := \frac{\mathrm{d}x^\mu}{\mathrm{d}\tau}, \quad x^0 = ct,\ x^1 = x. \tag{26}$$

Thus

$$u^0 = \gamma c, \quad u^1 = \gamma v. \tag{27}$$

Under the Minkowski metric $g_{\mu\nu} = \mathrm{diag}(-1, +1)$,

$$g_{\mu\nu} u^\mu u^\nu = -\gamma^2 c^2 + \gamma^2 v^2 = -\gamma^2 (c^2 - v^2) = -c^2, \tag{28}$$

recovering the standard four-velocity normalization.

Connection to Relativistic Energy Ratio.— The internal rate v_{int}/c connects directly to the relativistic energy ratio. In the low-energy regime $\mu\Delta t, pa \ll 1$, Taylor expansion of the dispersion relation (7) yields the Dirac dispersion $\omega^2(p) \approx \mu^2 + p^2 c^2$ (see Appendix A for detailed derivation). From the internal rate definition (18), we obtain

$$\frac{v_{\text{int}}(p)}{c} \approx \frac{\mu}{\omega(p)}. \tag{29}$$

Defining the physical mass via $mc^2 := \hbar\mu$ and physical energy $E(p) := \hbar\omega(p)$, this becomes

$$\frac{v_{\text{int}}(p)}{c} \approx \frac{mc^2}{E(p)}, \tag{30}$$

precisely the ratio of rest energy to total energy. With physical momentum $p_{\text{phys}} = \hbar p$, the Dirac dispersion yields the relativistic energy-momentum relation $E^2(p) \approx p_{\text{phys}}^2 c^2 + m^2 c^4$. Since in relativity $\mathrm{d}\tau/\mathrm{d}t = mc^2/E$, this exactly matches our definition (23), showing that the four-velocity normalization and time dilation follow from the geometric constraint Eq. (1). The information rate circle thus provides a compact geometric organization of relativistic kinematics within the Dirac QW, rather than an independent derivation of special relativity.

B. One-Step Entanglement Bound and Operational Meaning of v_{int}

The information rate circle Eq. (1) would remain a purely kinematic identity without operational significance if v_{int} were not linked to a physical observable. **The following result establishes such a link**: the internal rate $v_{\text{int}}(p)$ directly controls the rate of quantum correlation generation between coin and position degrees of freedom, connecting the geometric constraint to an experimentally measurable quantum information resource.

We consider the linear entropy $S_{\text{lin}} := 1 - \mathrm{Tr}\,\rho_c^2$ of the coin reduced density matrix, which for a global pure state quantifies the entanglement between coin and position. Proposition 1 rigorously establishes v_{int} as the dominant physical scale governing entanglement growth after a single time step.

Proposition 1 (One-step narrow-wave-packet entanglement bound). Consider a Dirac-type quantum walk satisfying A1–A3, and an initial product state

$$|\Psi_0\rangle = \int \mathrm{d}p\, f(p)\ |p\rangle \otimes |\chi\rangle\,, \tag{31}$$

where $f(p)$ is normalized, has variance σ_p^2, and is sharply peaked around p_0 with $\sigma_p a \ll 1$. Then, in the low-energy regime $\mu\Delta t,\ p_0 a \ll 1$, the coin-position linear entropy after one step satisfies

$$S_{\text{lin}}(1) \ \le\ 2\,\sigma_p^2\,\Delta t^2 \left[v_{\text{ext}}^2(p_0) + \kappa\, v_{\text{int}}^2(p_0)\right] + \mathcal{O}(\sigma_p^3), \tag{32}$$

where $\kappa = \mathcal{O}(1)$ is a dimensionless constant depending only on the energy regime. In particular, for modes with small group velocity $|v_{\text{ext}}(p_0)| \ll c$, the entanglement production per step is controlled by the internal rate, $S_{\text{lin}}(1) \lesssim \sigma_p^2 \Delta t^2 v_{\text{int}}^2(p_0)$, up to order-one numerical factors.

Proof: The evolved state after one step is $|\Psi_1\rangle = \int \mathrm{d}p\, f(p)\, U(p)\, |\chi\rangle \otimes |p\rangle$. Tracing out position gives the

reduced coin state

$$\rho_c(1) = \int \mathrm{d}p\, |f(p)|^2\, U(p)\, |\chi\rangle\, \langle\chi|\, U^\dagger(p), \tag{33}$$

with linear entropy

$$S_{\mathrm{lin}}(1) = 1 - \iint \mathrm{d}p\, \mathrm{d}p'\, |f(p)|^2 |f(p')|^2\, \left|\langle\chi|U^\dagger(p)U(p')|\chi\rangle\right|^2. \tag{34}$$

For narrow wavepackets with $|p - p'| \lesssim \sigma_p$, we expand $U^\dagger(p)U(p') = \exp[-i(p'-p)\,\partial_p K(p_0)] + \mathcal{O}((p'-p)^2)$, where $K(p) := \Omega(p)\hat{n}(p)\cdot\vec{\sigma}$. For any Hermitian 2×2 matrix $G = \|\partial_p K\|\,\hat{u}\cdot\vec{\sigma}$ (with $\hat{u}$ a unit vector), the overlap satisfies $1 - |\langle\chi|e^{-i\delta G}|\chi\rangle|^2 \le \sin^2(\delta\|\partial_p K\|) \le \delta^2\|\partial_p K\|^2$. Integrating over the product measure $|f(p)|^2|f(p')|^2$ and using $\mathbb{E}[(p'-p)^2] = 2\sigma_p^2$ for independent identically distributed p, p' yields

$$S_{\mathrm{lin}}(1) \le 2\sigma_p^2\, \|\partial_p K(p_0)\|^2 + \mathcal{O}(\sigma_p^3). \tag{35}$$

Computing $\partial_p K = (\partial_p\Omega)\hat{n}\cdot\vec{\sigma} + \Omega\,\partial_p\hat{n}\cdot\vec{\sigma}$, we find $\|\partial_p K\|^2 = (\partial_p\Omega)^2 + \Omega^2|\partial_p\hat{n}|^2$, where $\hat{n}\cdot\partial_p\hat{n} = 0$ by the unit-norm constraint. In the low-energy regime, $\partial_p\Omega = v_{\mathrm{ext}}\Delta t$ and $\Omega^2|\partial_p\hat{n}|^2 \le \kappa\,\Delta t^2 v_{\mathrm{int}}^2$ (see Appendix C for detailed derivation), yielding Eq. (32). □

Physical interpretation: The bound (32) shows that one-step entanglement generation is controlled by $\partial_p K$, the momentum derivative of the generator. This splits into two physical contributions:

(i) The v_{ext}^2 term arises from dispersion ($\partial_p\Omega$), which causes the wave packet to spread and different momentum components to acquire different dynamical phases, leading to momentum-dependent coin evolution.

(ii) The v_{int}^2 term arises from Bloch-axis twisting ($\partial_p\hat{n}$), which directly encodes how the coin rotation axis varies across the wave packet, causing different momentum components to undergo different coin rotations even at fixed time.

Thus, the internal rate v_{int} controls the second mechanism: the rate at which the generator's internal structure varies with momentum. This provides a quantitative link between the geometric decomposition Eq. (1) and a rigorously bounded, experimentally accessible entanglement measure.

Mass and Relativistic Dispersion.— In the rest frame $p = 0$, the dispersion relation (7) gives $\omega(0) \approx \mu$ for $\mu\Delta t \ll 1$. We **define** the physical rest mass m by $E_0 := \hbar\omega(0) = mc^2$, yielding $m = \hbar\mu/c^2$. The low-energy Taylor expansion (detailed in Appendix A) gives $\omega^2(p) \approx \mu^2 + p^2c^2$, which with physical momentum $p_{\mathrm{phys}} = \hbar p$ yields the relativistic energy-momentum relation:

$$E^2(p) \approx p_{\mathrm{phys}}^2 c^2 + m^2 c^4. \tag{36}$$

Higher-order corrections in $\mu\Delta t$ and pa encode lattice effects that break continuous Lorentz symmetry at high energies.

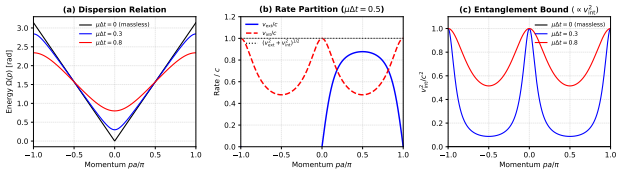

FIG. 2. Dispersion relation, velocity decomposition, and entanglement bound. (a) Dispersion relation $\Omega(p)$ for different mass parameters $\mu\Delta t$. The massless case ($\mu\Delta t = 0$, black) exhibits linear dispersion, while massive modes (blue, red) show characteristic gap opening at $p = 0$. (b) Velocity partition for intermediate mass ($\mu\Delta t = 0.5$): external group velocity v_{ext} (blue solid), internal rate v_{int} (red dashed), and their Pythagorean sum (black dotted, equal to c everywhere). (c) Entanglement generation proxy v_{int}^2/c^2 from Proposition 1. The massless mode (black) generates no coin-position entanglement, while massive modes exhibit peak entanglement generation near $p = 0$ (rest frame), directly demonstrating the operational significance of v_{int}.

This is the relativistic energy-momentum relation, derived purely from the QCA dispersion structure and the definition of mass as internal evolution rate.

Physical Interpretation.— The information rate circle provides a geometric reinterpretation of relativistic phenomena within this Dirac QW model:

Inertia: Mass resists acceleration because increasing external velocity requires decreasing internal rate (to preserve $v_{\mathrm{ext}}^2 + v_{\mathrm{int}}^2 = c^2$), which requires energy input proportional to the internal frequency μ (or equivalently, the physical mass $m = \hbar\mu/c^2$).

Time dilation: Moving particles age more slowly because their internal evolution rate $v_{\mathrm{int}} = c\sqrt{1 - v^2/c^2}$ decreases with external velocity v, directly defining proper time (23).

Light speed limit: Massless modes ($\mu = 0$) have $v_{\mathrm{int}} = 0$ and $v_{\mathrm{ext}} = c$, allocating the full geometric rate c to external propagation. Massive modes must have nonzero internal component, limiting $v_{\mathrm{ext}} < c$.

$E = mc^2$: Rest energy is the internal oscillation energy in the frame where external propagation vanishes.

C. Massless Limit and Lightlike Modes

The information rate circle provides a unified treatment of massive and massless Dirac modes. For $\mu = 0$, the coin rotation vanishes and the dispersion relation (7) reduces to

$$\cos\Omega(p) = \cos(pa). \tag{37}$$

At small momentum $pa \ll 1$, this gives $\Omega(p) \approx pa$, so $\omega(p) = \Omega/\Delta t \approx pa/\Delta t$, yielding the linear dispersion $E = \hbar\omega \approx \hbar cp$ characteristic of massless particles (with $p_{\mathrm{phys}} = \hbar p$).

From Eq. (18) we have

$$v_{\rm int}(p) = c\,\frac{\sin(\mu\Delta t)}{\sin\Omega(p)} = 0 \tag{38}$$

for $\mu = 0$, while Eq. (13) gives $v_{\rm ext}(p) = c\cos(\mu\Delta t)\sin(pa)/\sin\Omega(p) = c\,\mathrm{sgn}[\sin(pa)]$. Thus $|v_{\rm ext}| = c$ and $v_{\rm int} = 0$ for massless modes. The geometric quantity $v_{\rm int}$ vanishes, so the rate circle allocates all of the total geometric rate c to the group velocity, consistent with the kinematic property that null trajectories have vanishing proper time.

Clarification on internal dynamics: It is important to note that $v_{\rm int} = 0$ does *not* mean the coin degree of freedom is frozen. For $\mu = 0$, the generator $U(p) = e^{-ipa\hat{d}\cdot\vec{\sigma}}$ still induces nontrivial coin evolution for generic initial states; for instance, a superposition of eigenstates of $\hat{d}\cdot\vec{\sigma}$ will undergo Rabi oscillations with frequency proportional to pa. The vanishing of $v_{\rm int}$ is a *geometric statement* about the generator: the Bloch axis $\hat{n}(p)$ is aligned with the propagation direction $\hat{d}$, leaving no component in the "mass plane" orthogonal to $\hat{d}$. This alignment is what allows the full "update budget" c to be devoted to external propagation.

Conversely, for massive modes ($\mu \neq 0$), the requirement $v_{\rm int} > 0$ enforces $v_{\rm ext} < c$, providing a geometric interpretation for why particles with rest mass cannot reach light speed: the generator axis $\hat{n}(p)$ must have a nonzero component perpendicular to the propagation direction $\hat{d}$, limiting the group velocity.

D. Experimental Signatures and Parameter Estimates

The information rate circle predicts observable signatures in quantum simulation platforms where Dirac-type QCA can be implemented [11, 12].

Protocol 1: Verification via process tomography. Since $v_{\rm int}(p)$ is defined from the generator $U(p)$ rather than from time-evolved states, the natural experimental approach is:

(i) Use quantum process tomography [11] to reconstruct the single-step unitary $U(p_0)$ at a chosen momentum p_0. This requires applying U to a complete set of input states and performing state tomography on the outputs;

(ii) From the reconstructed $U(p_0)$, extract the SU(2) parameters $\Omega(p_0)$ and the Bloch axis $\hat{n}(p_0)$ by diagonalization or direct fitting;

(iii) With the known propagation direction $\hat{d}$ from the experimental design, compute $v_{\rm int}(p_0) = c\,|\hat{n}(p_0)\times\hat{d}|$ using the geometric formula;

(iv) Independently measure the group velocity $v_{\rm ext}(p_0)$ by preparing a wave packet localized around p_0 and tracking its center-of-mass motion: $v_{\rm ext} \approx \Delta\langle x\rangle/\Delta t$;

(v) Verify $v_{\rm ext}^2(p_0) + v_{\rm int}^2(p_0) = c^2$ within experimental error.

Noise sensitivity: Process tomography is resource-intensive ($\mathcal{O}(d^4)$ measurements for d-dimensional systems), but for two-level coins ($d = 2$) it is feasible with current trapped-ion [11] or superconducting-circuit platforms. Coherence times $T_2 \sim 1$ ms are sufficient for $\sim 10^2$ gate operations. Alternatively, if the update operator is known from the experimental design (as is typically the case), one can directly compute $v_{\rm int}$ from the programmed coin angle $\mu\Delta t$ and verify the circle relation using only the measured group velocity.

Typical parameters: For trapped ions with site spacing $a \sim 5\,\mu$m and time step $\Delta t \sim 10\,\mu$s, the maximal velocity scale is $c = a/\Delta t \sim 0.5$ m/s. A coin angle $\mu\Delta t \sim 0.1$ rad corresponds to a microscopic frequency $\mu \sim 10^4$ s^{-1}, yielding an effective mass $m = \hbar\mu/c^2 \sim 10^{-30}$ kg (or ~ 6 eV/c^2 in physical units). At lattice momentum $p \sim 0.1/a \sim 2\times10^4$ m^{-1}, both $v_{\rm ext}$ and $v_{\rm int}$ are of order ~ 0.3 m/s, well within experimental resolution.

Protocol 2: Mass from internal frequency. The relation $m = \hbar\mu/c^2$ can be tested by:

(i) Varying the coin rotation angle $\mu\Delta t$ across a range (e.g., 0.05 to 0.3 rad);

(ii) For each μ, measuring the rest-frame oscillation frequency $\omega(0)$ via spectroscopy of the Floquet quasienergy;

(iii) Verifying the relation $\omega(0) \approx \mu$ in the low-frequency regime $\mu\Delta t \ll 1$.

This directly tests the identification of physical mass with the internal frequency scale.

Protocol 3: Massless vs massive modes. By setting $\mu = 0$ (no coin rotation), one can realize massless Dirac-like excitations with $v_{\rm ext} = c$, $v_{\rm int} = 0$. Direct comparison with $\mu \neq 0$ modes demonstrates the geometric trade-off between external and internal rates.

Protocol 4: Multi-particle systems. Multi-particle quantum walks with interactions can probe corrections to the information rate geometry in the presence of effective gauge fields, providing a route toward simulating QED-like theories on QCA substrates.

II. DISCUSSION

A. Comparison with Previous Work

The connection between quantum walks (QW), quantum cellular automata (QCA), and the Dirac equation has been extensively studied [1, 5–7]. We summarize key prior results and clarify the novelty of the present work.

Existing results:

(i) Strauch (2006) [5] and Chandrashekar (2013) [6] showed that discrete-time quantum walks with appropriate coin operators yield Dirac-like effective Hamiltonians in the continuum limit $a, \Delta t \to 0$.

(ii) D'Ariano, Perinotti, and collaborators [1, 2] systematically constructed free quantum field theories (Dirac, Weyl, Maxwell) from QCA with specific symmetries, proving that QCA can serve as a discrete ontology for relativistic field theory.

(iii) Mallick and Chandrashekar (2016) [7] demonstrated explicit split-step QW realizations of Dirac cellular automata.

These works establish that Dirac dynamics emerges from QCA/QW in long-wavelength limits, but do not identify a *universal informational constraint* underlying the kinematic structure of special relativity.

Novelty of the present work:

Our contribution consists of three distinct advances:

(1) *Exact finite-lattice geometric identity.* Within the Dirac-type quantum walks defined by Eq. (3), we show that the single-step unitary $U(p) \in \mathrm{SU}(2)$ admits a natural decomposition: the group velocity and a complementary internal rate satisfy

$$\frac{v_{\mathrm{ext}}(p)}{c} = \hat{n}(p) \cdot \hat{d}, \qquad \frac{v_{\mathrm{int}}(p)}{c} = |\hat{n}(p) \times \hat{d}|, \tag{39}$$

where $\hat{n}(p)$ is the Bloch axis and $\hat{d}$ is the propagation direction. The unit-norm constraint $|\hat{n}(p)| = 1$ immediately yields $v_{\mathrm{ext}}^2(p) + v_{\mathrm{int}}^2(p) = c^2$. Mathematically, this is a simple consequence of SU(2) geometry. The physical significance lies in what follows.

(2) *Operational significance via entanglement generation.* We prove (Proposition 1) that v_{int} controls a rigorous upper bound on coin-position entanglement growth for narrow wave packets: $S_{\mathrm{lin}}(1) \le 2\sigma_p^2 \Delta t^2 [v_{\mathrm{ext}}^2 + \kappa v_{\mathrm{int}}^2]$. This establishes that v_{int} is not merely a geometric artifact but governs the rate of quantum information generation. Combined with the identification $c = v_{\mathrm{LR}}$ (Lieb-Robinson velocity), the rate circle becomes a decomposition of the causal light-cone speed into external propagation and internal correlation-generation components. This is the core new physical content of our work.

(3) *Relativistic kinematics as geometric organization.* The identity $v_{\mathrm{ext}}^2 + v_{\mathrm{int}}^2 = c^2$ provides a compact organization of known relativistic relations: defining proper time via $\mathrm{d}\tau = (v_{\mathrm{int}}/c)\,\mathrm{d}t$, the energy-momentum relation $E^2 = p^2c^2 + m^2c^4$, time dilation, and four-velocity normalization all follow as corollaries. Previous work derives these from dispersion relation analysis; we show they are geometric consequences of the SU(2) constraint together with the identification $v_{\mathrm{int}}/c \approx mc^2/E$.

(4) *Experimental protocols.* We provide explicit protocols for measuring v_{ext} and v_{int} simultaneously on existing quantum simulation platforms, with concrete parameter estimates for trapped-ion and superconducting-circuit implementations. This operational grounding distinguishes our approach from purely formal QCA-to-continuum mappings.

In summary, while existing work establishes the *feasibility* of deriving Dirac physics from discrete quantum dynamics, our work provides a compact geometric organization of relativistic kinematics within this Dirac QW class via the exact finite-lattice constraint $v_{\mathrm{ext}}^2 + v_{\mathrm{int}}^2 = c^2$, and demonstrates how to directly test this decomposition in quantum simulators.

B. Extensions and Future Directions

Geometric observation: Relation to Lieb-Robinson velocity. For the Dirac-type quantum walks studied in this paper, the lattice velocity scale $c = a/\Delta t$ plays a dual role: it is both (i) the single-particle massless group velocity and (ii) the Lieb-Robinson causal velocity v_{LR} for this nearest-neighbor QCA (see A2). The information rate circle Eq. (1) can thus be rewritten as $v_{\mathrm{ext}}^2(p) + v_{\mathrm{int}}^2(p) = v_{\mathrm{LR}}^2$, showing that the external and internal rates together saturate the causal light-cone speed.

One can ask whether a similar geometric constraint holds for more general two-level Floquet QCAs beyond the Dirac class. As a toy illustration, consider a translation-invariant QCA with local Hilbert space $\mathbb{C}^2$ per site, finite interaction range R, and single-particle sector $U(p) = e^{-i\Omega(p)\hat{n}(p)\cdot\vec{\sigma}}$. The Lieb-Robinson bound implies $|v_{\mathrm{ext}}(p)| := |\mathrm{d}\omega/\mathrm{d}p| \le v_{\mathrm{LR}}$ for all p [9]. For a chosen reference direction $\hat{d} \in S^2$, one can always define $v_{\mathrm{int}}(p) := v_{\mathrm{LR}}\,|\hat{n}(p) \times \hat{d}|$ and parametrize the group velocity as $v_{\mathrm{ext}}(p) = \eta(p)\, v_{\mathrm{LR}}\, (\hat{n} \cdot \hat{d})$ for some function $\eta(p) \in [-1, 1]$. Then, by the unit-norm constraint $|\hat{n}|^2 = 1$, one obtains

$$v_{\mathrm{ext}}^2(p) + v_{\mathrm{int}}^2(p) = v_{\mathrm{LR}}^2 \left[\eta^2 (\hat{n}\cdot\hat{d})^2 + |\hat{n}\times\hat{d}|^2\right] \le v_{\mathrm{LR}}^2, \tag{40}$$

with equality if and only if $|\eta(p)| = 1$ for all p. The Dirac-type walks of this paper achieve $\eta(p) \equiv 1$, thereby saturating the bound everywhere.

However, the physical content of this observation depends crucially on whether the parametrization $v_{\mathrm{ext}} = \eta\, v_{\mathrm{LR}}\, (\hat{n} \cdot \hat{d})$ is natural for a given model. For Dirac-type QCAs, this parametrization follows automatically from the dispersion relation; for other two-level QCAs, the relationship between v_{ext} and the Bloch geometry may be more complicated, and the choice of $\hat{d}$ less canonical. We therefore regard the above as a *geometric reparametrization* that clarifies the special status of Dirac walks (they saturate $v_{\mathrm{ext}}^2 + v_{\mathrm{int}}^2 = v_{\mathrm{LR}}^2$) rather than as a general theorem applicable to all Floquet QCAs. A systematic classification of which two-level QCA models admit such a rigid parametrization is an interesting question for future work.

Higher-dimensional generalization. We expect an analogous sphere constraint to hold in higher-dimensional Dirac-type QCA models, where $\vec{v}_{\mathrm{ext}} \in \mathbb{R}^d$ collects the components of the group velocity. A

schematic illustration is provided by the separable model

$$U(\vec{p}) = C(\mu) \prod_{j=1}^{d} T_j(p_j), \tag{41}$$

where $T_j(p_j) = \exp(-ip_j a\sigma_j)$ and the dispersion relation becomes $\cos\Omega(\vec{p}) = \cos(\mu\Delta t)\prod_{j=1}^{d}\cos(p_j a)$. In this toy example, the external velocity vector $\vec{v}_{\text{ext}} = (\partial\omega/\partial p_1, \ldots, \partial\omega/\partial p_d)$ and internal velocity would satisfy

$$|\vec{v}_{\text{ext}}|^2 + v_{\text{int}}^2 = c^2. \tag{42}$$

However, a rigorous construction of Dirac-type QCA in $d > 1$ spatial dimensions requires careful treatment of spinor representations and gamma-matrix structures [1], which may lead to modifications of this simple sphere constraint. Equation (42) should therefore be regarded as an illustrative example rather than a general theorem in higher dimensions. A full analysis is beyond the scope of this work and is left for future investigation.

Interacting theories and gauge fields. Interactions and gauge fields modify the dispersion structure [13]. For example, minimal coupling to a U(1) gauge field corresponds to replacing $p_j \to p_j - eA_j/\hbar c$ in the translation operators, which deforms the information rate geometry. The constraint (42) becomes coordinate-dependent, with local variations encoding electromagnetic forces.

Extension to curved spacetime. The extension to curved spacetime requires understanding how local variations in QCA structure—e.g., site-dependent coin angles $\mu(x)$, coupling strengths, or lattice geometry—induce effective metric geometry. Preliminary analysis suggests that spatially varying parameters can encode optical-type metrics, providing a route to quantum simulation of general-relativistic phenomena. This is a direction we are currently pursuing.

A fundamental question remains: *Why does nature choose QCA with parameters satisfying A1–A3?* One possibility is that these axioms are not independent but follow from deeper consistency conditions, analogous to how Lorentz invariance follows from locality and causality in quantum field theory. Another possibility is that multiple QCA "universe models" exist, with observable physics selecting a particular class.

Regardless of these foundational questions, the information rate circle establishes a rigorous correspondence, within the Dirac QCA setting analyzed here, between discrete quantum-information dynamics and the kinematic structure of continuous relativistic geometry. Crucially, this correspondence is not merely formal: the internal rate v_{int} controls a measurable quantum resource—coin-position entanglement generation (Proposition 1)—demonstrating that the geometric constraint has direct operational significance in quantum information processing. This suggests that spacetime is not a primitive entity but an emergent description of information flow patterns in quantum systems with finite local information capacity.

ACKNOWLEDGMENTS

The author thanks [to be specified] for discussions on quantum cellular automata and quantum walk experiments.

Appendix A: Low-Energy Expansion and Relativistic Dispersion

Here we provide the detailed Taylor expansion used in the main text to derive the Dirac dispersion $\omega^2(p) \approx \mu^2 + p^2c^2$ from the exact lattice dispersion relation.

From the dispersion relation (7), $\cos\Omega(p) = \cos(\mu\Delta t)\cos(pa)$, in the low-energy regime $\mu\Delta t, pa \ll 1$, we expand:

$$\cos\Omega(p) \approx 1 - \frac{\Omega^2}{2} + \mathcal{O}(\Omega^4), \tag{A1}$$

$$\cos(\mu\Delta t) \approx 1 - \frac{(\mu\Delta t)^2}{2} + \mathcal{O}((\mu\Delta t)^4), \tag{A2}$$

$$\cos(pa) \approx 1 - \frac{(pa)^2}{2} + \mathcal{O}((pa)^4). \tag{A3}$$

Substituting and expanding the product to second order:

$$\begin{aligned}\cos(\mu\Delta t)\cos(pa) &\approx \left(1 - \frac{(\mu\Delta t)^2}{2}\right)\left(1 - \frac{(pa)^2}{2}\right) \\ &\approx 1 - \frac{(\mu\Delta t)^2}{2} - \frac{(pa)^2}{2} + \mathcal{O}((\mu\Delta t)^2(pa)^2).\end{aligned} \tag{A4}$$

Equating with the expansion of $\cos\Omega$ yields

$$\Omega^2(p) \approx (\mu\Delta t)^2 + (pa)^2. \tag{A5}$$

Dividing by Δt^2 and using $c = a/\Delta t$:

$$\omega^2(p) = \frac{\Omega^2(p)}{\Delta t^2} \approx \mu^2 + p^2c^2. \tag{A6}$$

With physical energy $E = \hbar\omega$, physical momentum $p_{\text{phys}} = \hbar p$, and mass $m = \hbar\mu/c^2$, this yields

$$E^2(p) \approx p_{\text{phys}}^2 c^2 + m^2c^4. \tag{A7}$$

Appendix B: SU(2) Multiplication and Bloch Axis Derivation

The single-step update operator in the Dirac-QCA model is

$$U(p) = C(\mu)T(p) = e^{-i\mu\Delta t\hat{m}\cdot\vec{\sigma}}e^{-ipa\hat{d}\cdot\vec{\sigma}}, \tag{B1}$$

where $\hat{m}, \hat{d} \in S^2$ are orthogonal unit vectors ($\hat{m}\cdot\hat{d} = 0$). Both factors are elements of SU(2).

The product of two SU(2) elements satisfies [10]

$$e^{-i\alpha\hat{a}\cdot\vec{\sigma}}e^{-i\beta\hat{b}\cdot\vec{\sigma}} = e^{-i\gamma\hat{c}\cdot\vec{\sigma}}, \tag{B2}$$

where the composition angle γ is determined by

$$\cos\gamma = \cos\alpha\cos\beta - (\hat{a}\cdot\hat{b})\sin\alpha\sin\beta. \tag{B3}$$

For our choice $\hat{a} = \hat{m}$, $\hat{b} = \hat{d}$, $\alpha = \mu\Delta t$, $\beta = pa$, with $\hat{m}\cdot\hat{d} = 0$, we have

$$\cos\gamma = \cos(\mu\Delta t)\cos(pa). \tag{B4}$$

Identifying $\gamma = \Omega(p)$ yields the dispersion relation (7).

The Bloch axis $\hat{c}$ satisfies

$$\hat{c}\sin\gamma = \hat{a}\sin\alpha\cos\beta + \hat{b}\sin\beta\cos\alpha - (\hat{a}\times\hat{b})\sin\alpha\sin\beta. \tag{B5}$$

Substituting our parameters gives

$$\hat{n}(p)\sin\Omega(p) = \hat{m}\sin(\mu\Delta t)\cos(pa) + \hat{d}\sin(pa)\cos(\mu\Delta t) - (\hat{m}\times\hat{d})\sin(\mu\Delta t)\sin(pa), \tag{B6}$$

recovering Eq. (8). This is the basis-independent vector form of the Bloch axis.

To extract components in the natural frame $\{\hat{e}_1 = \hat{m}, \hat{e}_2 = -\hat{m}\times\hat{d}, \hat{e}_3 = \hat{d}\}$, we note that $\hat{m} = \hat{e}_1$, $\hat{d} = \hat{e}_3$, and $\hat{m}\times\hat{d} = \hat{e}_1\times\hat{e}_3 = -\hat{e}_2$. Substituting into the vector equation above and comparing coefficients of $\hat{e}_j$ yields

$$n_1\sin\Omega = \sin(\mu\Delta t)\cos(pa), \tag{B7}$$
$$n_2\sin\Omega = \sin(\mu\Delta t)\sin(pa), \tag{B8}$$
$$n_3\sin\Omega = \cos(\mu\Delta t)\sin(pa), \tag{B9}$$

which are Eqs. (10)–(12).

Geometric verification of the information rate circle.— From the group velocity derivation, we have $v_{\rm ext}/c = n_3 = \hat{n}\cdot\hat{d}$. To verify the cross-product form of $v_{\rm int}$, we compute

$$\hat{n}\times\hat{d} = (n_1\hat{e}_1 + n_2\hat{e}_2 + n_3\hat{e}_3)\times\hat{e}_3 = n_1(\hat{e}_1\times\hat{e}_3) + n_2(\hat{e}_2\times\hat{e}_3) = -n_1\hat{e}_2 + n_2\hat{e}_1 \tag{B10}$$

where we used $\hat{e}_1\times\hat{e}_3 = -\hat{e}_2$ and $\hat{e}_2\times\hat{e}_3 = \hat{e}_1$. Therefore,

$$|\hat{n}\times\hat{d}| = \sqrt{n_1^2 + n_2^2} = \frac{v_{\rm int}}{c}. \tag{B11}$$

The information rate circle then follows immediately from the standard vector identity: for any unit vector $\hat{n}$ and any fixed direction $\hat{d}$,

$$(\hat{n}\cdot\hat{d})^2 + |\hat{n}\times\hat{d}|^2 = |\hat{n}|^2|\hat{d}|^2 = 1, \tag{B12}$$

which upon multiplication by c^2 yields $v_{\rm ext}^2 + v_{\rm int}^2 = c^2$.

Appendix C: Algebraic Verification of Information Rate Circle

We provide an independent algebraic verification of the information rate circle that complements the geometric proof in the main text.

From the dispersion relation $\cos\Omega = \cos(\mu\Delta t)\cos(pa)$, we have

$$\sin^2\Omega = 1 - \cos^2(\mu\Delta t)\cos^2(pa). \tag{C1}$$

From Eqs. (10)–(12), the Bloch axis components in the natural frame satisfy

$$n_1 = \frac{\sin(\mu\Delta t)\cos(pa)}{\sin\Omega}, \tag{C2}$$
$$n_2 = \frac{\sin(\mu\Delta t)\sin(pa)}{\sin\Omega}, \tag{C3}$$
$$n_3 = \frac{\cos(\mu\Delta t)\sin(pa)}{\sin\Omega}. \tag{C4}$$

By definition,

$$v_{\rm ext} = c\,n_3 = c\,\frac{\cos(\mu\Delta t)\sin(pa)}{\sin\Omega}, \tag{C5}$$

$$v_{\rm int} = c\sqrt{n_1^2 + n_2^2} = c\,\frac{\sin(\mu\Delta t)}{\sin\Omega}\sqrt{\cos^2(pa) + \sin^2(pa)} = c\,\frac{\sin(\mu\Delta t)}{\sin\Omega}. \tag{C6}$$

Therefore,

$$\begin{aligned} v_{\rm ext}^2 + v_{\rm int}^2 &= c^2\,\frac{\cos^2(\mu\Delta t)\sin^2(pa) + \sin^2(\mu\Delta t)}{\sin^2\Omega} \\ &= c^2\,\frac{\cos^2(\mu\Delta t)\sin^2(pa) + \sin^2(\mu\Delta t)[\cos^2(pa) + \sin^2(pa)]}{\sin^2\Omega} \\ &= c^2\,\frac{\cos^2(\mu\Delta t)\sin^2(pa) + \sin^2(\mu\Delta t)\cos^2(pa) + \sin^2(\mu\Delta t)\sin^2(pa)}{\sin^2\Omega} \\ &= c^2\,\frac{\sin^2(pa)[\cos^2(\mu\Delta t) + \sin^2(\mu\Delta t)] + \sin^2(\mu\Delta t)\cos^2(pa)}{\sin^2\Omega} \\ &= c^2\,\frac{\sin^2(pa) + \sin^2(\mu\Delta t)\cos^2(pa)}{\sin^2\Omega}. \end{aligned} \tag{C7}$$

Now observe that

$$\begin{aligned} &\sin^2(pa) + \sin^2(\mu\Delta t)\cos^2(pa) \\ &= [1 - \cos^2(pa)] + \sin^2(\mu\Delta t)\cos^2(pa) \\ &= 1 - \cos^2(pa)[1 - \sin^2(\mu\Delta t)] \\ &= 1 - \cos^2(pa)\cos^2(\mu\Delta t) \end{aligned}$$

Substituting back yields $v_{\rm ext}^2 + v_{\rm int}^2 = c^2$, completing

the algebraic verification.

Appendix D: Detailed Derivation of Entanglement Bound

Here we provide the complete derivation of the narrow-wave-packet entanglement bound (Proposition 1), including all explicit inequalities and constants.

The evolved state after one step is

$$|\Psi_1\rangle = \int \mathrm{d}p\, f(p)\, U(p)\, |\chi\rangle \otimes |p\rangle\,. \tag{D1}$$

Tracing out the position degree of freedom gives the reduced coin state

$$\rho_c(1) = \int \mathrm{d}p\, |f(p)|^2\, U(p)\, |\chi\rangle\, \langle\chi|\, U^\dagger(p). \tag{D2}$$

Its linear entropy is

$$S_{\mathrm{lin}}(1) = 1 - \mathrm{Tr}\,\rho_c^2(1) = 1 - \iint \mathrm{d}p\, \mathrm{d}p'\, w(p) w(p')\, \big|\langle\chi|U^\dagger(p) U(p')|\chi\rangle\big|^2, \tag{D3}$$

where $w(p) = |f(p)|^2$.

We now assume that $w(p)$ is sharply peaked around p_0 with variance σ_p^2 and expand $U^\dagger(p)U(p')$ for p, p' in this narrow window. Writing

$$K(p) := \Omega(p)\, \hat{n}(p) \cdot \vec{\sigma}, \qquad U(p) = e^{-iK(p)}, \tag{D4}$$

we have

$$U^\dagger(p)U(p') = e^{iK(p)} e^{-iK(p')} = \exp\big[-i(p'-p)\, \partial_p K(p_0)\big] + \mathcal{O}\big((p'-p)^2\big). \tag{D5}$$

Denote $G := \partial_p K(p_0)$ and $\delta := p' - p$. In the narrow-wave-packet regime $|\delta| \lesssim \sigma_p$ we can approximate $U^\dagger(p)U(p') = e^{-i\delta G} + \mathcal{O}(\delta^2)$.

For any Hermitian 2×2 matrix G we can write $G = g\, \hat{u} \cdot \vec{\sigma}$ with $g = \|G\|$ the operator norm and $\hat{u}$ a unit vector. Then $e^{-i\delta G} = e^{-i\delta g\, \hat{u}\cdot\vec{\sigma}}$ is a rotation on the Bloch sphere by angle $2\delta g$ around axis $\hat{u}$. For any pure coin state $|\chi\rangle$ one has the inequality

$$1 - \big|\langle\chi|e^{-i\delta G}|\chi\rangle\big|^2 \le \sin^2(\delta g) \le \delta^2 g^2, \tag{D6}$$

where the first inequality follows from the fact that the maximal deviation is achieved when $|\chi\rangle$ is an equal superposition of the eigenstates of G, and the second inequality follows from $\sin x \le x$.

Substituting (D6) into the exact expression (D3), and neglecting terms of order $\mathcal{O}(\delta^3)$, gives

$$\begin{aligned} S_{\mathrm{lin}}(1) &\le \iint \mathrm{d}p\, \mathrm{d}p'\, w(p) w(p')\, \delta^2\, \|G\|^2 + \mathcal{O}(\sigma_p^3) \\ &= \|G\|^2\, \mathbb{E}[(p'-p)^2] + \mathcal{O}(\sigma_p^3), \end{aligned} \tag{D7}$$

where the expectation value is with respect to the product measure $w(p)w(p')$. Since p and p' are independent and identically distributed,

$$\mathbb{E}[(p'-p)^2] = \mathbb{E}[p'^2] + \mathbb{E}[p^2] - 2\mathbb{E}[p]\mathbb{E}[p'] = 2\sigma_p^2. \tag{D8}$$

Thus

$$S_{\mathrm{lin}}(1) \le 2\sigma_p^2\, \|G\|^2 + \mathcal{O}(\sigma_p^3). \tag{D9}$$

It remains to bound $\|G\|$ in terms of v_{ext} and v_{int}. Using

$$G = \partial_p K(p_0) = (\partial_p \Omega)\, \hat{n} \cdot \vec{\sigma} + \Omega\, \partial_p \hat{n} \cdot \vec{\sigma}, \tag{D10}$$

we have

$$\|G\|^2 = (\partial_p \Omega)^2 + \Omega^2\, |\partial_p \hat{n}|^2, \tag{D11}$$

where we used $|\hat{n}| = 1$ and $\hat{n} \cdot \partial_p \hat{n} = 0$ to eliminate cross terms.

For the Dirac walk one has $\partial_p \Omega = \Delta t\, v_{\mathrm{ext}}(p_0)$ from the dispersion relation. In the low-energy regime $\mu\Delta t, p_0 a \ll 1$, a direct differentiation of Eqs. (10)–(12) in the main text shows that

$$|\partial_p \hat{n}(p_0)| \le \kappa'\, a\, \frac{\sin(\mu\Delta t)}{\sin^2 \Omega(p_0)} = \kappa'\, \frac{a}{c}\, \frac{v_{\mathrm{int}}(p_0)}{c}, \tag{D12}$$

for some numerical constant $\kappa' = \mathcal{O}(1)$. Using $c = a/\Delta t$ and the fact that $\Omega(p_0) = \mathcal{O}(1)$ in the regime of interest, we can rewrite this as

$$\Omega^2(p_0)\, |\partial_p \hat{n}(p_0)|^2 \le \kappa\, \Delta t^2\, v_{\mathrm{int}}^2(p_0), \tag{D13}$$

for another order-one constant κ.

Substituting these estimates into (D11) yields

$$\|G\|^2 \le \Delta t^2 \Big[v_{\mathrm{ext}}^2(p_0) + \kappa\, v_{\mathrm{int}}^2(p_0) \Big]. \tag{D14}$$

Combining with (D9) proves the desired bound.

[1] G. M. D'Ariano and P. Perinotti, *Quantum cellular automata and free quantum field theory*, Phys. Rev. A **90**, 062106 (2014).

[2] A. Bisio, G. M. D'Ariano, and P. Perinotti, *Quantum cellular automaton theory of light*, Ann. Phys. **368**, 177 (2016).

[3] T. A. Brun et al., *Quantum cellular automata and quantum field theory in two spatial dimensions*, Phys. Rev. A **102**, 062222 (2020).

[4] L. S. Trezzini, *Renormalisation of quantum cellular au-*

tomata, (unpublished).

[5] F. W. Strauch, *Relativistic quantum walks*, Phys. Rev. A **73**, 054302 (2006).

[6] C. M. Chandrashekar, *Two-component Dirac-like Hamiltonian for generating quantum walk on one-, two- and three-dimensional lattices*, Sci. Rep. **3**, 2829 (2013).

[7] A. Mallick and C. M. Chandrashekar, *Dirac cellular automaton from split-step quantum walk*, Sci. Rep. **6**, 25779 (2016).

[8] E. H. Lieb and D. W. Robinson, *The finite group velocity of quantum spin systems*, Commun. Math. Phys. **28**, 251 (1972).

[9] B. Nachtergaele and R. Sims, *Much ado about something: why Lieb–Robinson bounds are useful*, J. Stat. Phys. **124**, 1 (2006).

[10] J. J. Sakurai and J. Napolitano, *Modern Quantum Mechanics*, 2nd ed. (Cambridge University Press, 2017).

[11] C. H. Alderete et al., *Quantum walks and Dirac cellular automata on a trapped-ion quantum computer*, npj Quantum Inf. **6**, 89 (2020).

[12] N. P. Kumar and C. M. Chandrashekar, *Bounds on the dynamics of periodic quantum walks and emergence of the gapless and gapped Dirac equation*, Phys. Rev. A **97**, 012116 (2018).

[13] T. A. Brun et al., *Quantum electrodynamics from quantum cellular automata*, (unpublished).